Cooper Union for the Advancement of Science and Art

Final - Design of a Compressor

ME-407: Computational Fluid Dynamics

Authors:
Michelle Meiner
Preston Xu
Benjamin Meiner
Neil Sawhney

Professor:
Professor Bondi

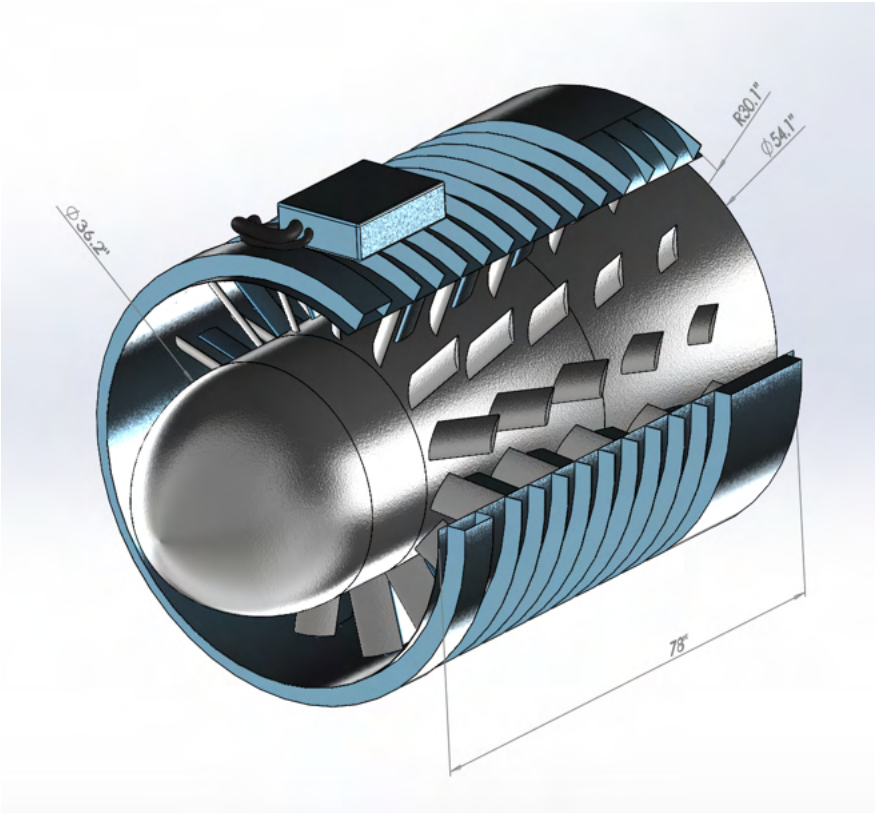

July 12, 2024

Contents

1 Objective

The objective is to design the compressor stage for a gas turbofan engine to compress the intake air before it is delivered to the combustion chamber. The goal is to optimize the efficiency of the compressor through analysis of its ideal geometry, number of stages, and speed of each stage.

1.1 Model Requirements

The compressor must reach a minimum pressure ratio of 22:1 at the maximum design altitude of 40,000 ft. It's outer diameter must remain within 4'-6' and it can run at a maximum of 40000 rpm.

1.2 Model Assumptions

1. The model is tested on a test stand which simulates the standard pressure at the required altitude. All simulations are done at the standard temperature, pressure, and density conditions of air at 40,000 ft.
2. The compressor is modeled without a gap between the blade and the shroud because this gap was assumed to be negligible compared to the effects of the rest of the geometry.
3. The model assumes that each stage will rotate perfectly uniformly, however, there would likely be inconsistencies during operation.
4. The construction will be made of Nickel Alloy because of its very high melting point and desirable structural properties.

1.3 Pressure Ratio

The desired pressure ratio is 22:1. Therefore, the desired outlet pressure is calculated using Equation 4. The starting pressure is atmospheric pressure at 40,000 feet which according to *Engineering Toolbox* corresponds to a pressure of 0.1845 atm.

$$P_{out} = P_{ratio} * P_{inlet} \tag{1}$$
$$P_{out} = 22 * (0.1845atm) \tag{2}$$
$$P_{out} = 4.059atm \tag{3}$$
$$\tag{4}$$

Therefore at 40,000 ft, the outlet total pressure must reach 4.059 atm.

2 Hand Calculations

To verify the CFD results to follow, ballpark hand calculations must be performed. Hand calculations will be used to estimate the output temperature and efficiency of the compressor. In Section 6, these hand calculations will be compared with simulation results.

2.1 Temperature

The outlet temperature is found using the combined ideal gas law from *Professional Engineer Mechanical Handbook* as shown in Equation 8. At 40,000 ft the temperature is -70 °F according to *Engineering Toolbox*.

$$\frac{P_1 * V_1}{T_1} = \frac{P_2 * V_2}{T_2} \tag{5}$$

$$T_2 = \frac{P_2 * V_2 * T_1}{P_1 * V_1} \tag{6}$$

$$T_2 = \frac{22 * 0.25ft^2 * 216.5K}{1 * 0.84ft^2} \tag{7}$$

$$T_2 = 2062°F \tag{8}$$

At 40,000 ft, the outlet temperature is expected to be 2062 °F.

2.2 Efficiency

A ballpark calculation for input energy to spin the rotor is necessary to estimate the 1st law efficiency of the compressor, i.e. input fan energy (power required to rotate the rotor due to drag and or lift of the blade) versus pressure ratio. The outer diameter of the rotor is measured to be 60" at its biggest, and 36" at its smallest, to achieve a ballpark estimate, the average of these diameters will be used at 48". The speed that the rotor's foil moves through the air can then be calculated as a function of the rpm using the following equation:

$$v = \frac{2\pi r N}{60} \tag{9}$$

where

v = velocity of the foil through the air (ft/s)

r = radius of the rotor (ft)

N = rpm of the rotor (rpm)

The angle of the rotors foil with the free stream velocity is 40 degrees or 0.7 radians. The lift and drag forces can be calculated by using a flat plate foil theory. The majority of the drag and lift will be from the rotors. The stators act to remove the circulation of air after each rotor such that the next rotor experiences a free stream velocity similar to that at the compressor inlet. We will assume that the stators are working properly and can therefore simplify the analysis to a single rotor. The pressure drop from one rotor will then be multiplied by the number of necessary rotors to achieve the compression ratio. The lift and drag forces are given by the following equations from *Fundamentals of Aerodynamics*.

$$L = \frac{1}{2}\rho v^2 A C_L \tag{10}$$

$$D = \frac{1}{2}\rho v^2 A C_D \tag{11}$$

where

L = lift force (lbf)

D = drag force (lbf)

ρ = density of air (lbm/ft^3)

v = velocity of the foil through the air (ft/s)

A = area of the foil (ft^2)

C_L = lift coefficient

C_D = drag coefficient

$C_L = 2\pi\alpha$

$C_D = 1.28C_L^2$

The projected area of the foil is measured to be 68.4 in^2 Plugging in the values for the lift and drag forces and air properties at 40,000 ft from *Engineering Toolbox*, we get the lift and drag on the foil as a function of rpm N as shown in Equation 13 and Equation 15.

$$L = 0.5 \times (0.043 lb/ft^3) \times \left(\frac{2\pi \times 48in \times N}{60}\right)^2 \times (68.4in^2) \times 2\pi \times 0.7 \tag{12}$$

$$L = 68 * 10^{-9} N^2 lbf \tag{13}$$

$$D = 0.5 \times (0.043 lb/ft^3) \times \left(\frac{2\pi \times 48in \times N}{60}\right)^2 \times (68.4in^2) \times 2\pi \times 0.314 \times 1.28 \times (2\pi \times 0.7)^2 \tag{14}$$

$$D = 756 * 10^{-9} N^2 lbf \tag{15}$$

We can convert to an ideal pressure drop by dividing the lift by the projected area of the foil.

$$\Delta P = \frac{L}{A * cos(\alpha)} \tag{16}$$

$$\Delta P = \frac{68 * 10^{-9} N^2 lbf}{(68.4in^2) * cos(0.7)} \tag{17}$$

$$\Delta P = 1.3 * 10^{-9} N^2 lbf/in^2 \tag{18}$$

Because there are 15 blades on one stage of the rotor, the total pressure drop is 15 times the pressure drop of one blade times the number of rotor stages M. The total pressure drop is then given by the following equation.

$$\Delta P_{total} = 15 \times 1.3 * 10^{-9} N^2 M lbf/in^2 \tag{19}$$

The power output from the pressure drop can be calculated by multiplying the pressure by the change in area by the velocity as shown in Equation 20. The change in area is calculated by subtracting the outlet area from the inlet area for each rotor stage. This change is approximately 127 in^2.

$$P_{output} = v \times P_{total} \times (127in^2) \tag{20}$$

The power required to rotate the rotor is governed by the following equation which computes the component of the drag and lift force that opposes the rotation of the rotor.

$$P_{input} = v \times (Dcos(\alpha) + Lsin(\alpha)) * N * M \tag{21}$$

where

D = drag force (lbf)
L = drag force (lbf)
v = velocity of the foil through the air (ft/s)
N = Number of rotors
M = Number of rotor stages

The efficiency of the rotor can then be calculated by dividing the power output by the power input as shown in Equation 24. As will be shown in later sections, the chosen rpm was 20,000 with 6 rotor stages.

$$\eta = \frac{P_{total} \times (127in^2)}{(Dcos(\alpha) + Lsin(\alpha)) * N * M} \tag{22}$$

$$\eta = \frac{6 * 10^3 lbf}{((302.4lbf)cos(0.7) + (27.2lbf)sin(0.7)) * (120000)} \tag{23}$$

$$\eta = 0.201 \tag{24}$$

The expected efficiency for our design is therefore 20.1%

3 Geometry

3.1 Airfoil Blades

The rotor blade uses a NACA-6412 airfoil at a 40 degree angle of attack and the stator blade is a NACA-3012 airfoil oriented parallel to the wall (no angle of attack).

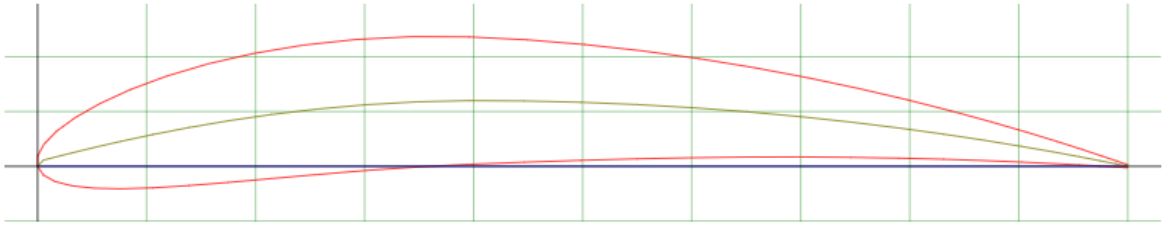

(a) NACA 6412 Rotor blade airfoil

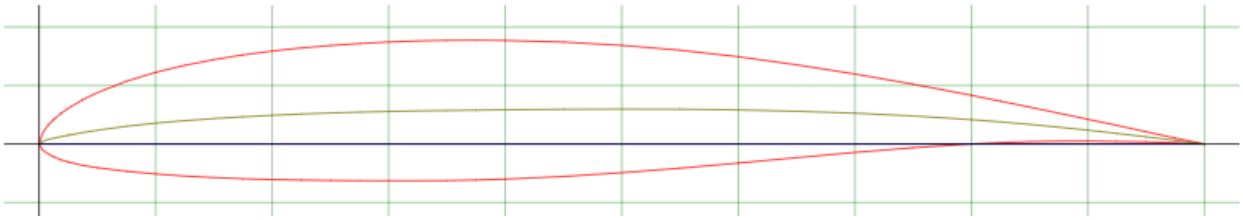

(b) NACA-3012 Stator blade airfoil

Figure 3.1: Airfoils Comparison for Rotor and Stator

3.2 Design

The compressor has five stages, each containing a rotor and a stator with a decreasing cross sectional area across the model. The blades are 24 degrees away from each other allowing for a total of 15 blades per section. Each rotor operates at the same angular velocity, 20,000 RPM as decided in Section 6. To simulate the compressor in fluent, the air around one row of blades was used.

The bounding box of the compressor is 60" x 78". All other dimensions are shown in detail in the technical drawing shown in Appendix A.1

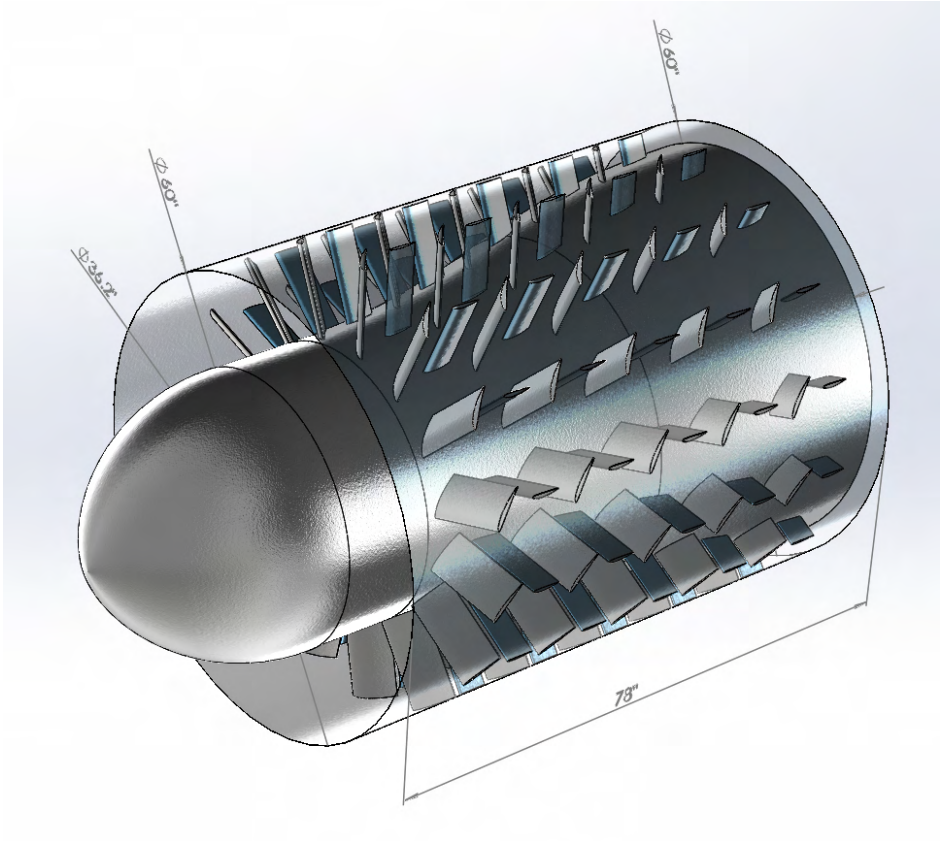

Figure 3.2: CAD of Compressor. Grey-Rotor, Blue Translucent Stator. Units in inches.

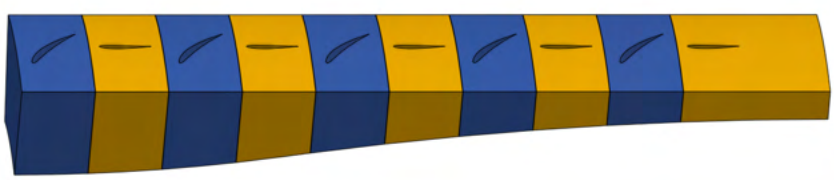

Figure 3.3: CAD of Air. Blue-Rotor, Orange-Stator

4 Mesh

Hypermesh was used to discretize the geometry. The mesh, shown in Figure 4.1 is fully mapped, consisting of only hexahedral and pyramidal elements. The mesh was refined near the blades because they will experience large gradients in pressure and velocity and are therefore of special interest. The mesh contains 1.5 million elements. The average element size (the length of an elements edge) around the rotors is 0.08 inches and the average element size everywhere else is 0.24 inches. The boundary layer around the blades has a first layer thickness of 0.03 inches with a growth rate of 1.2.

While the mesh could have been made by sweeping elements radially outwards, this creates poor element quality around the blades and creates some elements with extremely small orthogonality. Instead, the geometry was sliced on both sides of the blades on the YZ plane (as referenced by Figure 4.1) and the elements were swept linearly in the z direction. The side faces on the XZ plane were then 2D meshed and swept in the Y direction for each rotor and stator.

4.1 Mesh Quality

All metrics such as aspect ratio, cell size, orthogonality, and warpage are well within acceptable limits as shown in Table 1.

Table 1: Mesh Quality Criteria

Criterion	**Minimum**	**Maximum**
Cell Size (inches)	3×10^{-6}	0.04
Aspect Ratio	1	13
Orthogonality	0.3	1
Warpage	0	0.6
Jacobian	0.8	1
Cell Squish	0.005	0.07

Because the mesh is fully mapped, all the elements have exceptional quality. These metrics are visualized in Figure 4.2 to highlight the areas of better and worse quality for each metric. The aspect ratio is of course higher near the walls of the blades due to the nature of the boundary layer and the cell size is smaller due to the increase in resolution. The orthogonality is very good throughout the model, especially in the high resolution areas of interest.

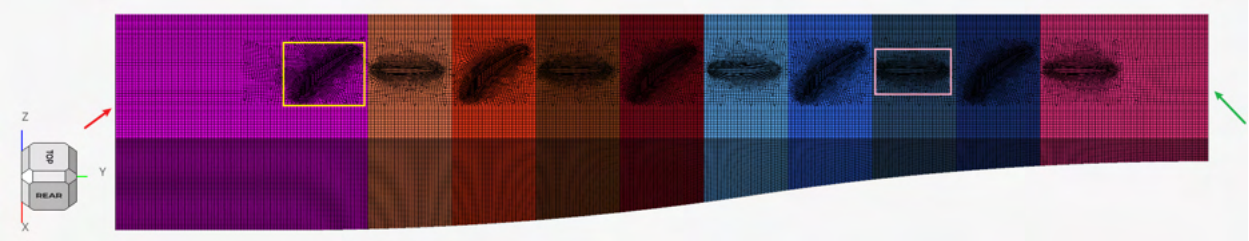

(a) Side View of the Mesh

fluid_rotor_1	31
fluid_rotor_2	32
fluid_rotor_3	33
fluid_rotor_4	34
fluid_rotor_5	35
fluid_stator_1	36
fluid_stator_2	37
fluid_stator_3	38
fluid_stator_4	39
fluid_stator_5	40

(b) Fluid Domain Coloring

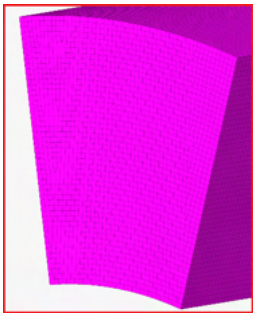

(c) **Zoom:** Inlet

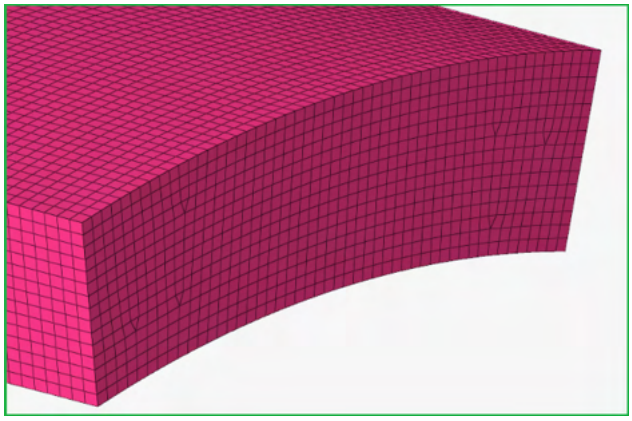

(d) **Zoom:** Outlet

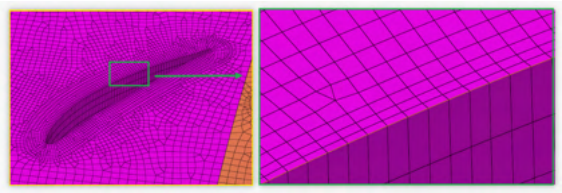

(e) **Zoom:** First Rotor **Ultra Zoom:** Boundary Layer

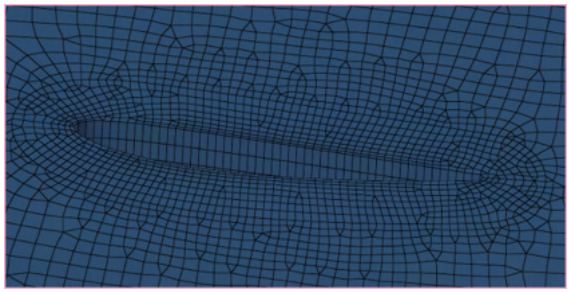

(f) **Zoom:** Fourth Stator

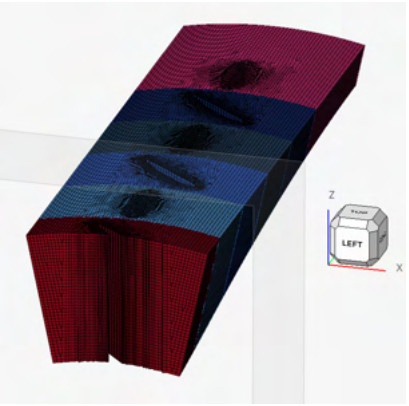

(g) Section Cut View on the XZ Plane

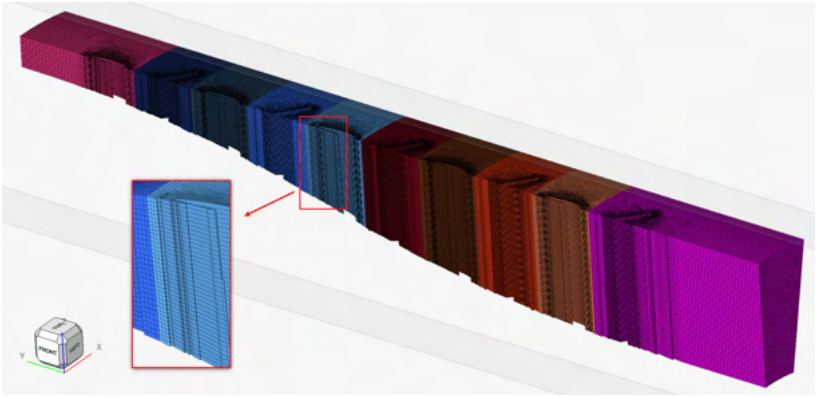

(h) Section Cut View on the YZ Plane with Zoomed in View of Stator 3

Figure 4.1: Mapped mesh of the compressor. Subplots 4.1c - 4.1f contain zoomed in areas of 4.1a organized by border color. The mesh is a mix of hexahedral and pyramidal elements. The average element size around the rotors is 0.08 inches and the average element size everywhere else is 0.24 inches. The boundary layer around the blades has a first layer thickness of 0.03 in with a growth rate of 1.2.

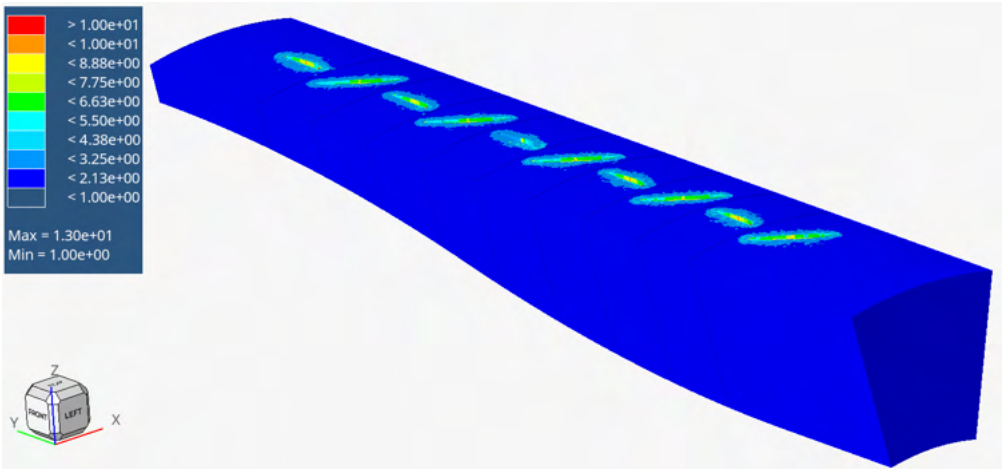

(a) Aspect Ratio

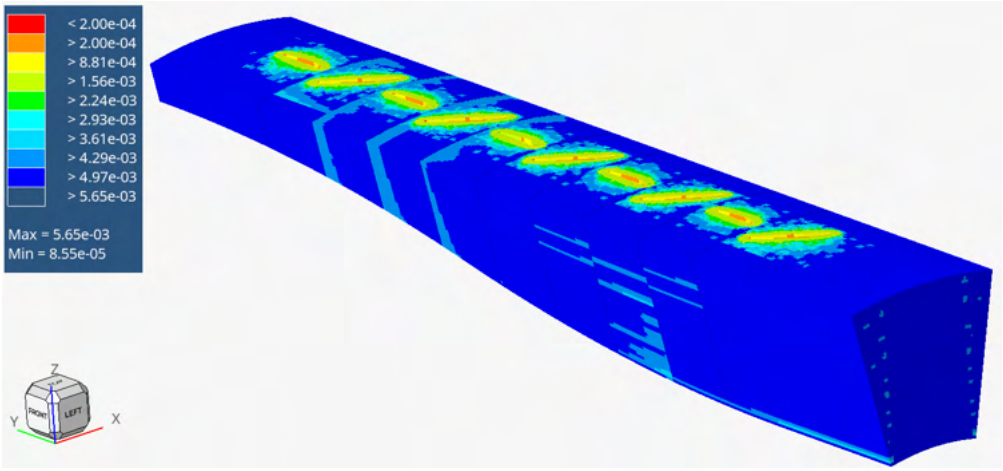

(b) Cell Size
The units are in meters. When converted to inches, the minimum cell size is 3.3e-6 inches and the maximum cell size is 0.04 inches.

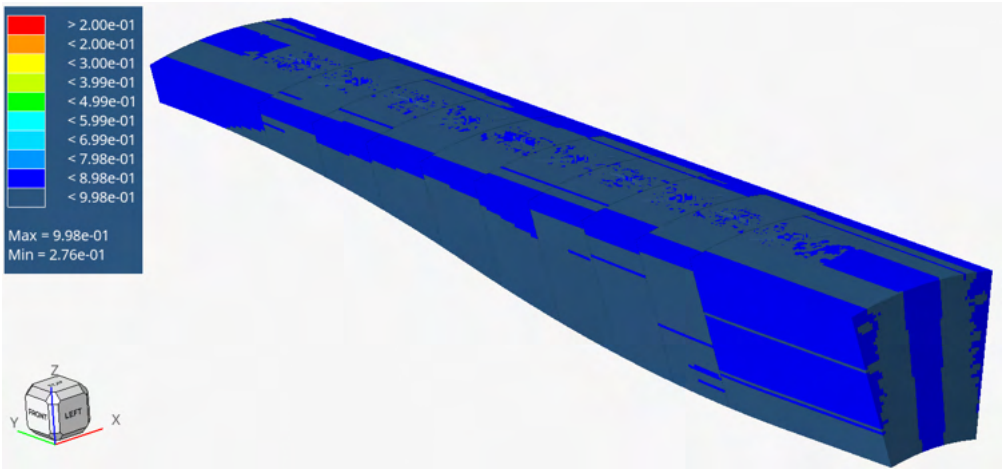

(c) Orthogonality

Figure 4.2: Mesh Quality Metrics in Hypermesh.

5 Model Setup in Ansys Fluent

The transient solver in Ansys Fluent was used for solving. Fluent allows for rotational periodic conditions which allows one section of the blade to simulate results for the whole compressor since the geometry is radially symmetric. Since compressors are designed to compress air, an ideal gas law condition was used to allow the density of air to change throughout the model. The sliding mesh motion method was used with each rotor section starting off with a speed of 10,000 RPM and was increased after convergence. The operating condition was set to 0.1845 atm, standard pressure at 40,000 ft.

5.0.1 Boundary Conditions

A pressure inlet and outlet were used. For the pressure inlet, the gauge pressure was set to zero and the temperature was set to -70 F, the standard temperature at 40,000 ft. The outlet gauge pressure was set to zero gauge will an 100 F back flow temperature.

5.0.2 Mesh Interfaces

A periodic repeat interface was set at each of the interfaces between the rotor and stator which caused the blades to slide past one another in a circle. Periodic boundary interfaces were set between the right and left hand side of each rotor and stator which allowed these walls to perform as if they were adjacent blades. These as well as all other boundary conditions are shown in Figure 5.1.

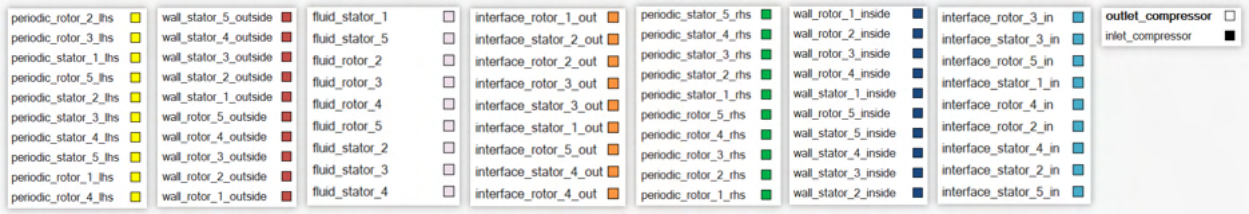

(a) Boundary Condition Names

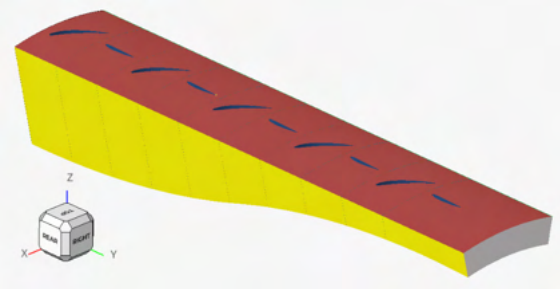

(b) Top Isometric View

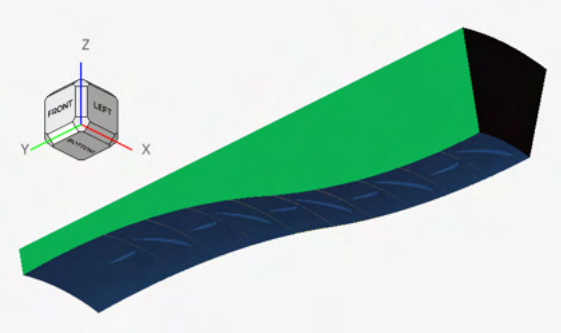

(c) Bottom Isometric View

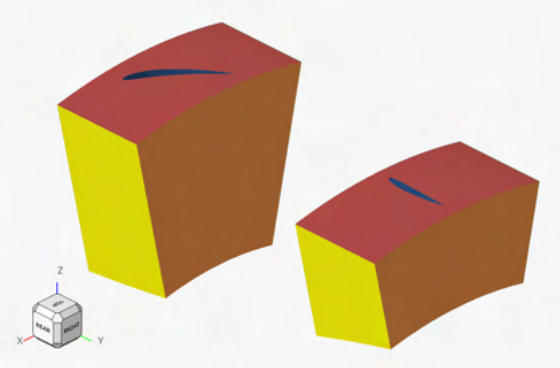

(d) Isolated Top View of Rotor 2 and Stator 3

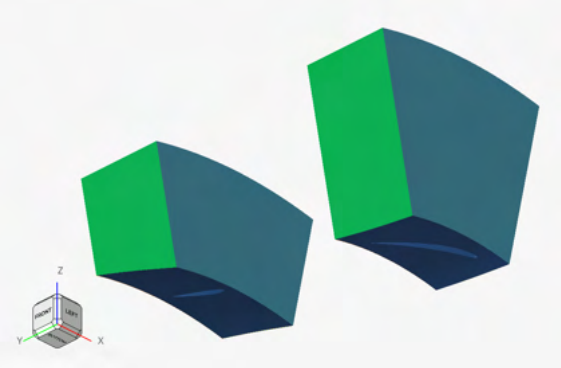

(e) Isolated Bottom View of Rotor 2 and Stator 3

Figure 5.1: Boundary conditions of the compressor created in Hypermesh. The Boundary's are created using the Faces tool and named according to Figure 5.1a. Subplots 5.1d and 5.1e hide the majority of the geometry to show the interfaces between the rotor and stator.

5.0.3 Time Step

Depending on the RPM of the blade, the time step was set up so that the sliding meshes would never skip a cell within one time step. For 10,000 RPM, $6e^{-10}s$ was used and for 20,000 RPM, $4e^{-10}s$ was used. Each time step included 20 iterations, but it typically converged between eight and thirteen iterations.

5.1 Operating Altitude (40,000 ft)

The SIMPLE scheme was used and the inviscid model for turbulence was used to help convergence. For the spatial discretization, least squares cell based was used for the gradient, second order for pressure, and first order upwind for density, momentum, and energy. The total pressure, mass flow rate, and temperature at the outlet were monitored during the simulation and are shown in Section 5.1.1.

5.1.1 Operating Altitude (40,000 ft) Simulation Convergence

For each simulation, the continuity residual was below 10^{-2} while the others were below 10^{-5}. The residuals for the 10K RPM simulation are shown in Figure 5.2. The system's periodic nature is evident, with each period corresponding to the passing of the blades. Figure 5.2 shows convergence plots for the 10,000 RPM case.

Because the pressure ratio is still well under the desired 22:1, the model was run at 20,000 RPM to see if the pressure ratio would increase. Figure 5.3 shows the convergence plots after the additional 20,000 RPM iterations.

5.3 shows that while the total pressure seems converged at 20,000 RPM, the outlet temperature is still rising and the mass flow is still divergent. Unfortunately the simulation crashed at this point and refused to start back up from this iteration. Therefore, the results are used anyway since the total pressure is of the most importance and seems reasonably converged.

5.2 Operation at Sea Level

Although the design point was at 40,000 ft, the model was also run at sea level to see how the compressor would perform at a lower altitude. The same boundary conditions and solver settings were used except for pressure at the inlet which was set to 1 atm.

5.2.1 Sea Level Simulation Convergence

For each simulation, the continuity residual was below 10^{-2} while the others were below 10^{-5}. The residuals for the 20K RPM simulation at standard temperature and pressure are shown in Figure 5.4. Convergence plots are shown in figure 5.4.

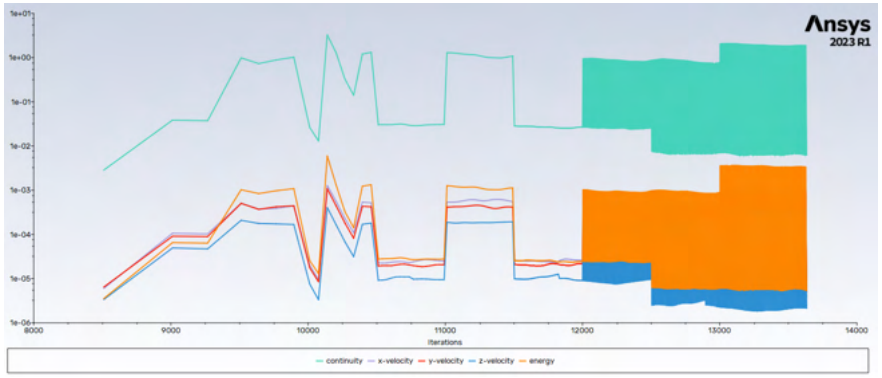

(a) Residuals

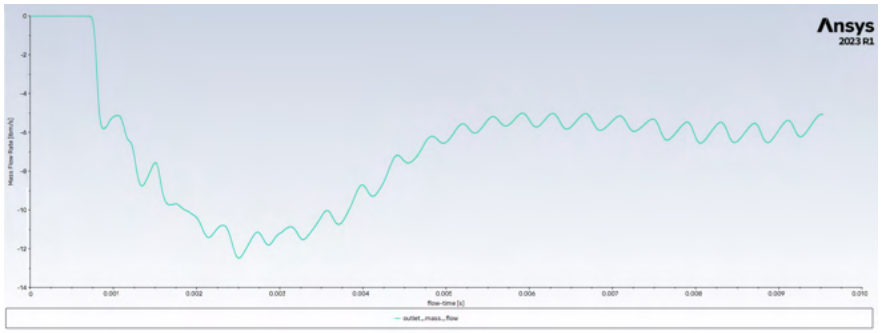

(b) Outlet Mass Flow

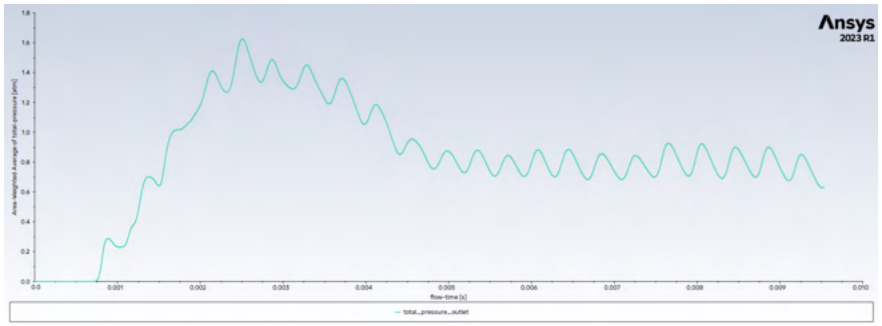

(c) Total Pressure Outlet

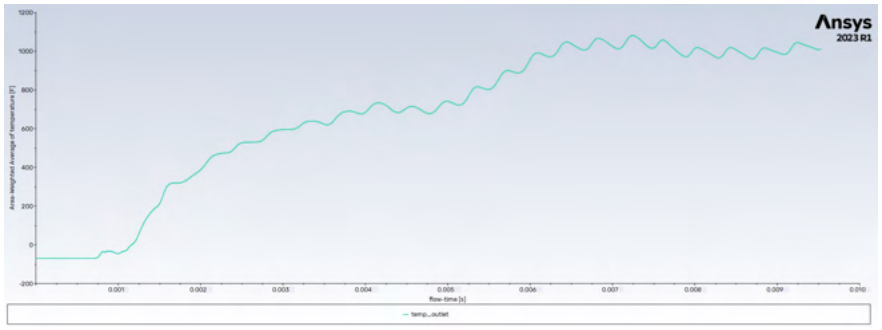

(d) Temperature Outlet

Figure 5.2: Convergence Plots for 10,000 RPM Simulation at 40,000 ft

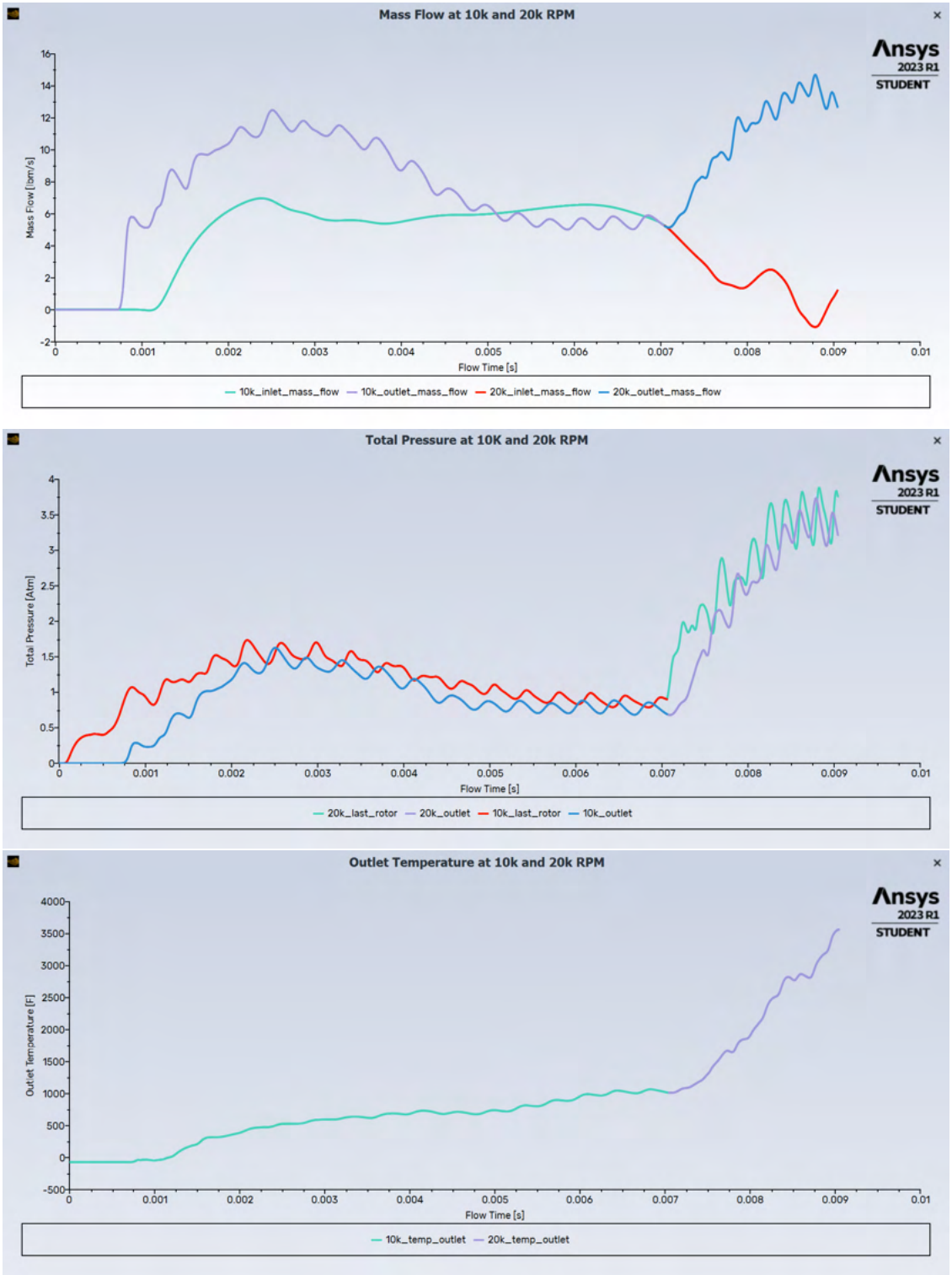

Figure 5.3: Convergence Plots for 10,000 and 20,000 RPM Simulations at 40,000 ft: The Total Pressure and Outlet Temperature plots are computed using an area weighted average.

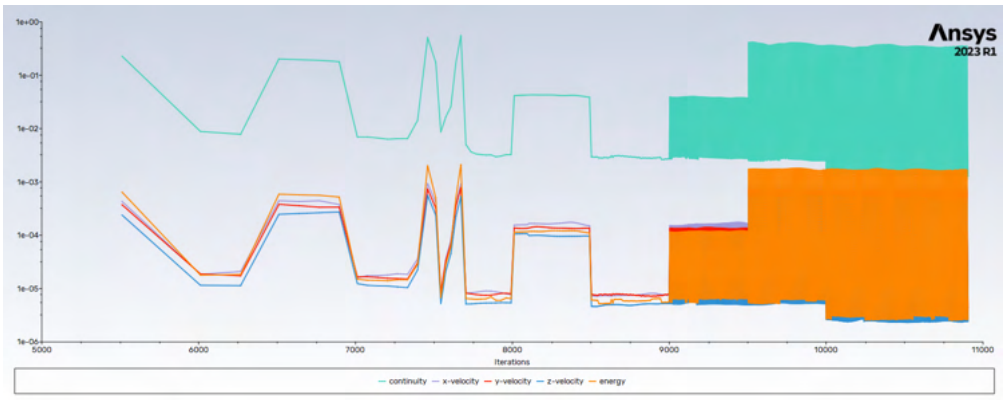

(a) Residuals

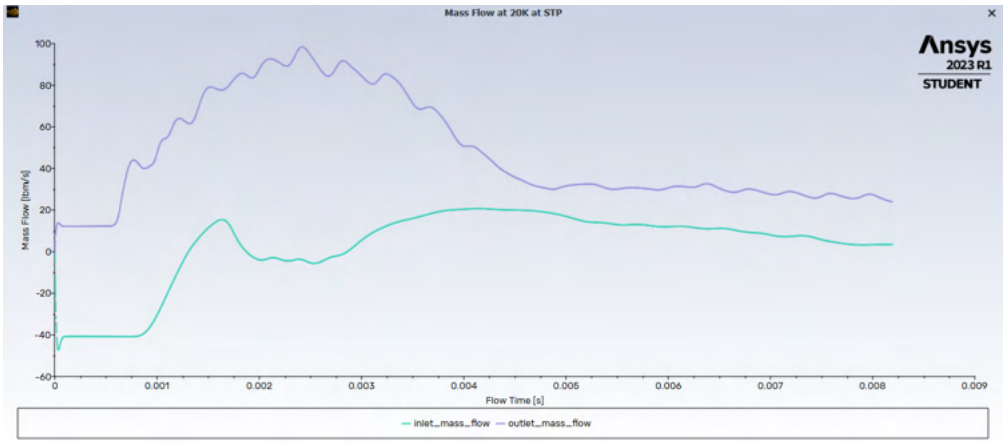

(b) Mass Flow

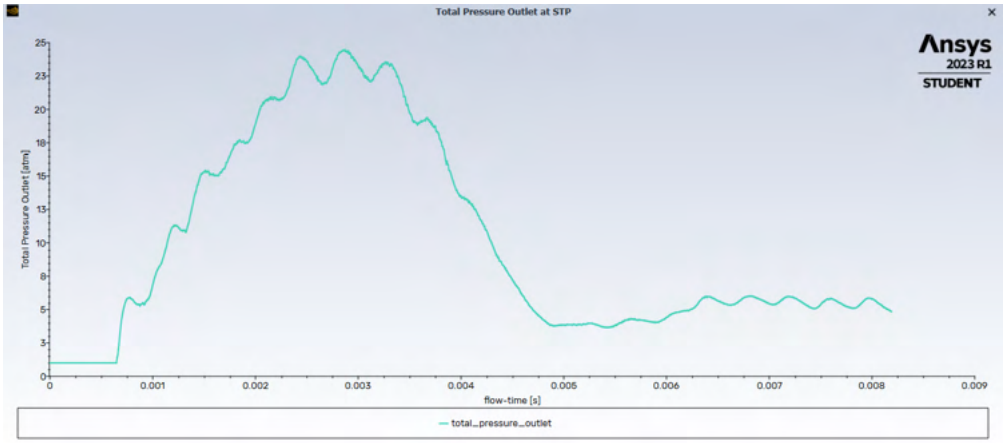

(c) Total Pressure

Figure 5.4: Convergence Plots for 20,000 RPM Simulation at Sea Level

6 Results

Because all the rotors spin together, the pressure is highest when the stators and rotors align and lowest when they are most staggered. This causes a steady oscillation in monitored parameters at convergence. Each result will be displayed at the low point during the last cycle of oscillation, however, these will then be averaged with the results at the high point during the last cycle of oscillation in all the tabulated results.

6.1 Sea Level Simulation Results

6.1.1 Temperature Contours

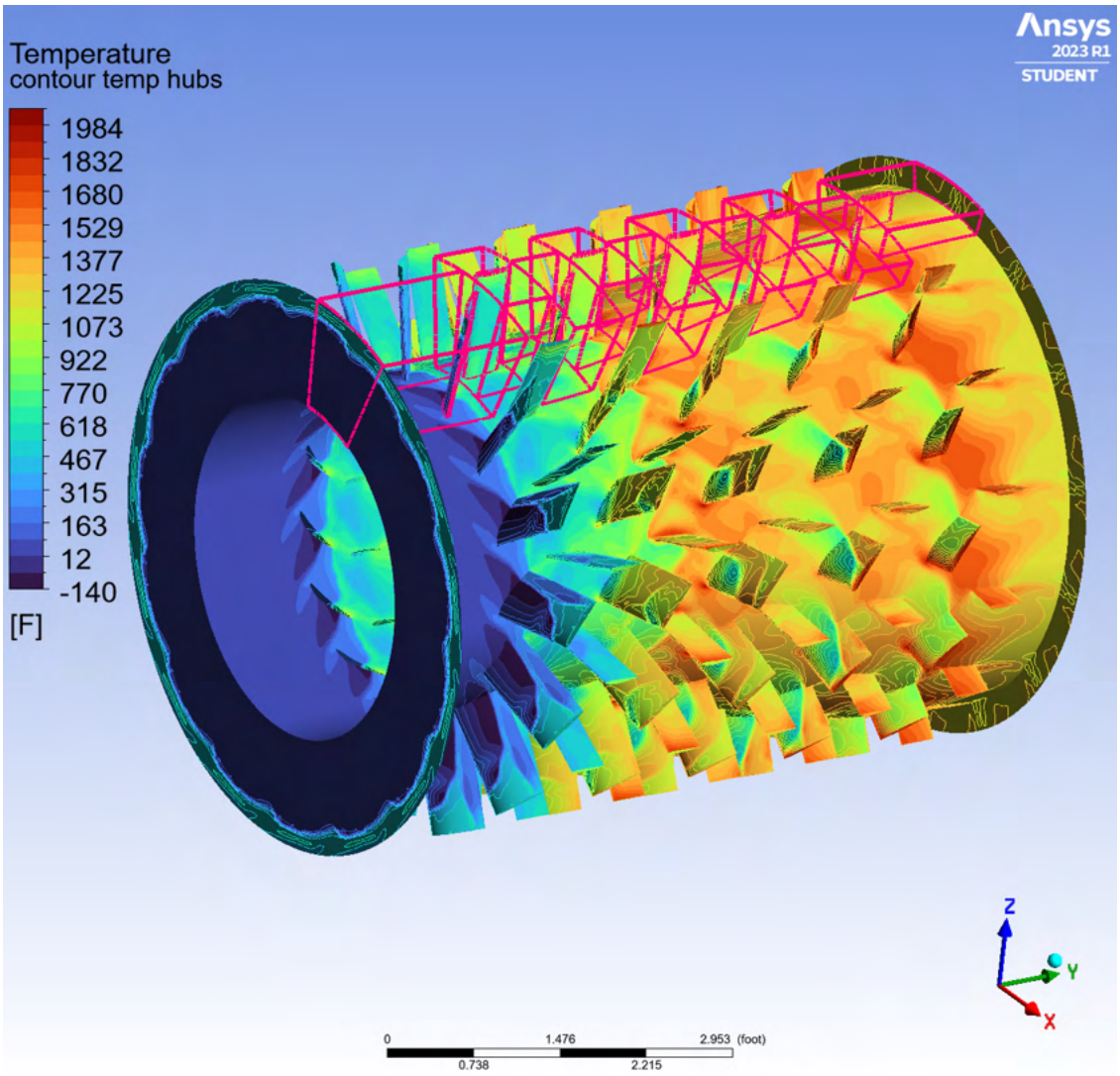

The temperature is highest right behind the last rotor at around 1800 degrees which is just under the melting point of the nickel alloy construction. However, this is on a test stand and shell conduction is turned off. In reality, convection from the moving plane would help cool the engine, and the conduction throughout the metal would help distribute the temperature more evenly.

6.1.2 Velocity Streamlines

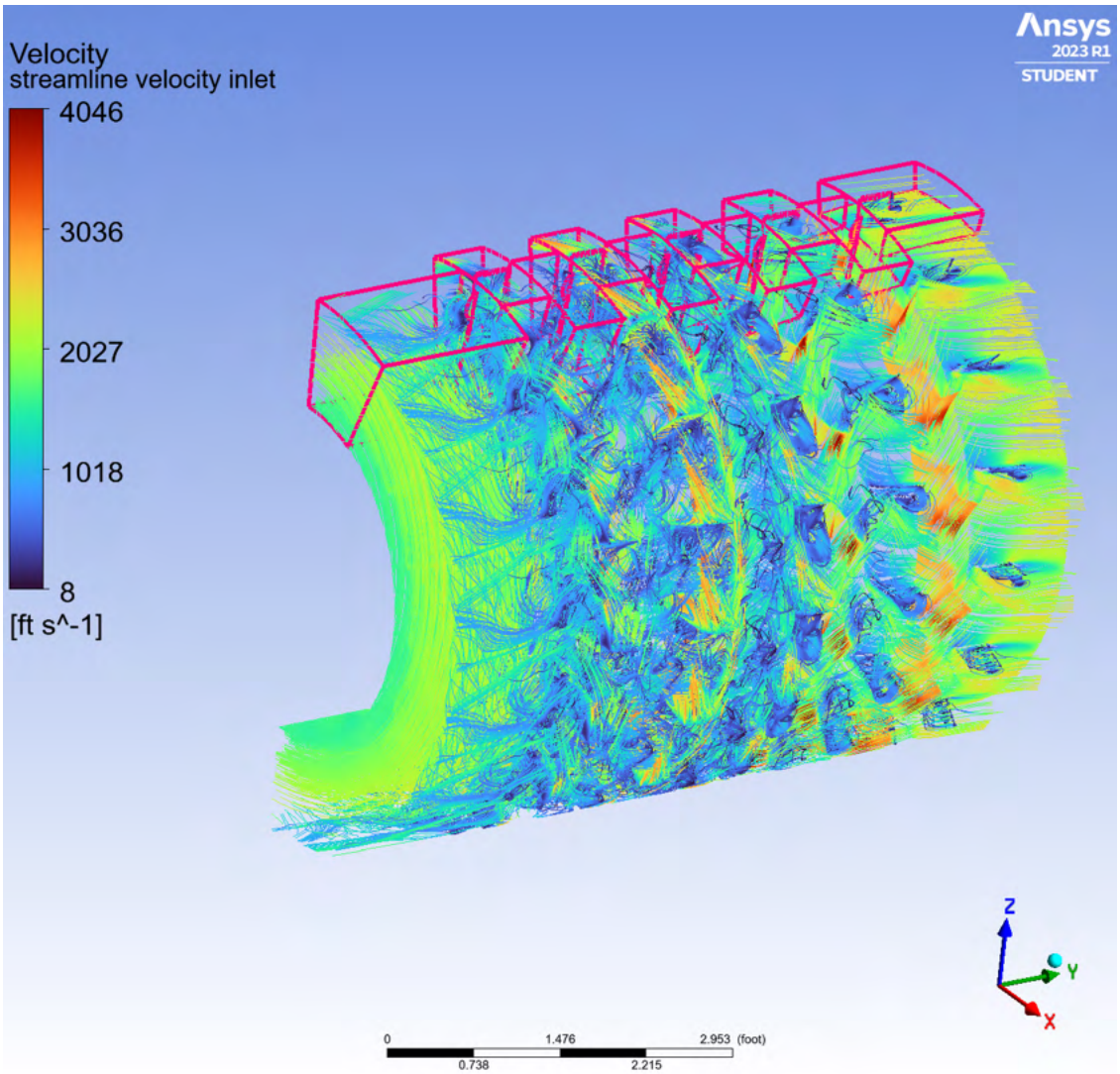

The velocity is highest at the outlet of the last rotor, although overall the velocity is fairly consistent. The velocity is taken with respect to the inertial frame and is expressed in the inertial frame. This is why the velocity is very low near the walls, despite the fact that the rotors are spinning very quickly. As expected the velocity increases towards the outlet of the compressor.

6.1.3 Pressure Contours

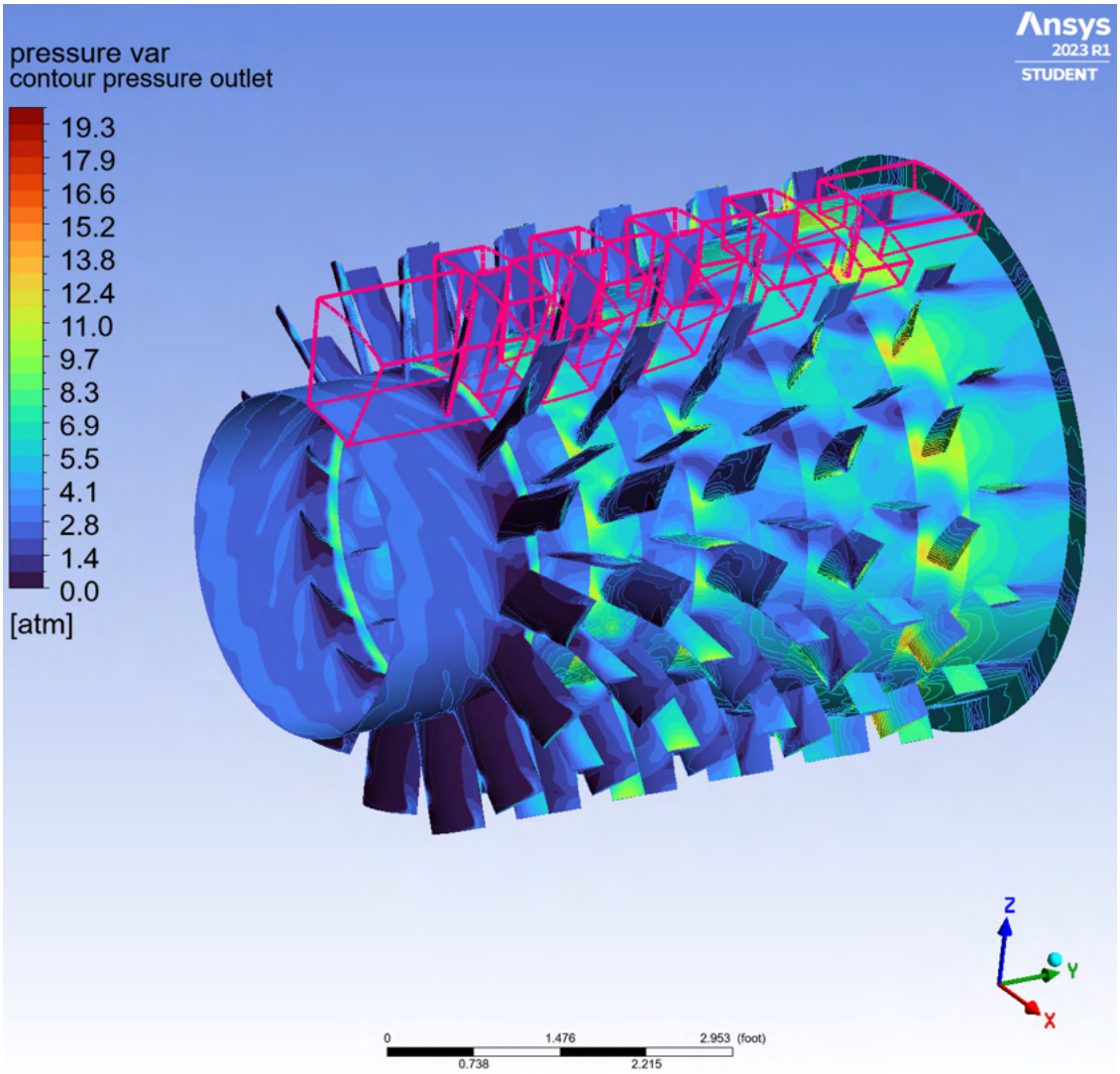

The pressure ratio is highest on the leading edge of the the last rotor, and is less on each of the stators. This makes sense because the rotors are spinning very quickly relative to the fluid so it is expected that the rotors should experience greater pressure.

6.1.4 Pressure Ratio

The pressure ratio, sometimes called the compression ratio, is calculated at standard temperature and pressure using Equation 25.

$$P_{ratio} = \frac{P_{out} + 1atm}{1atm} \tag{25}$$

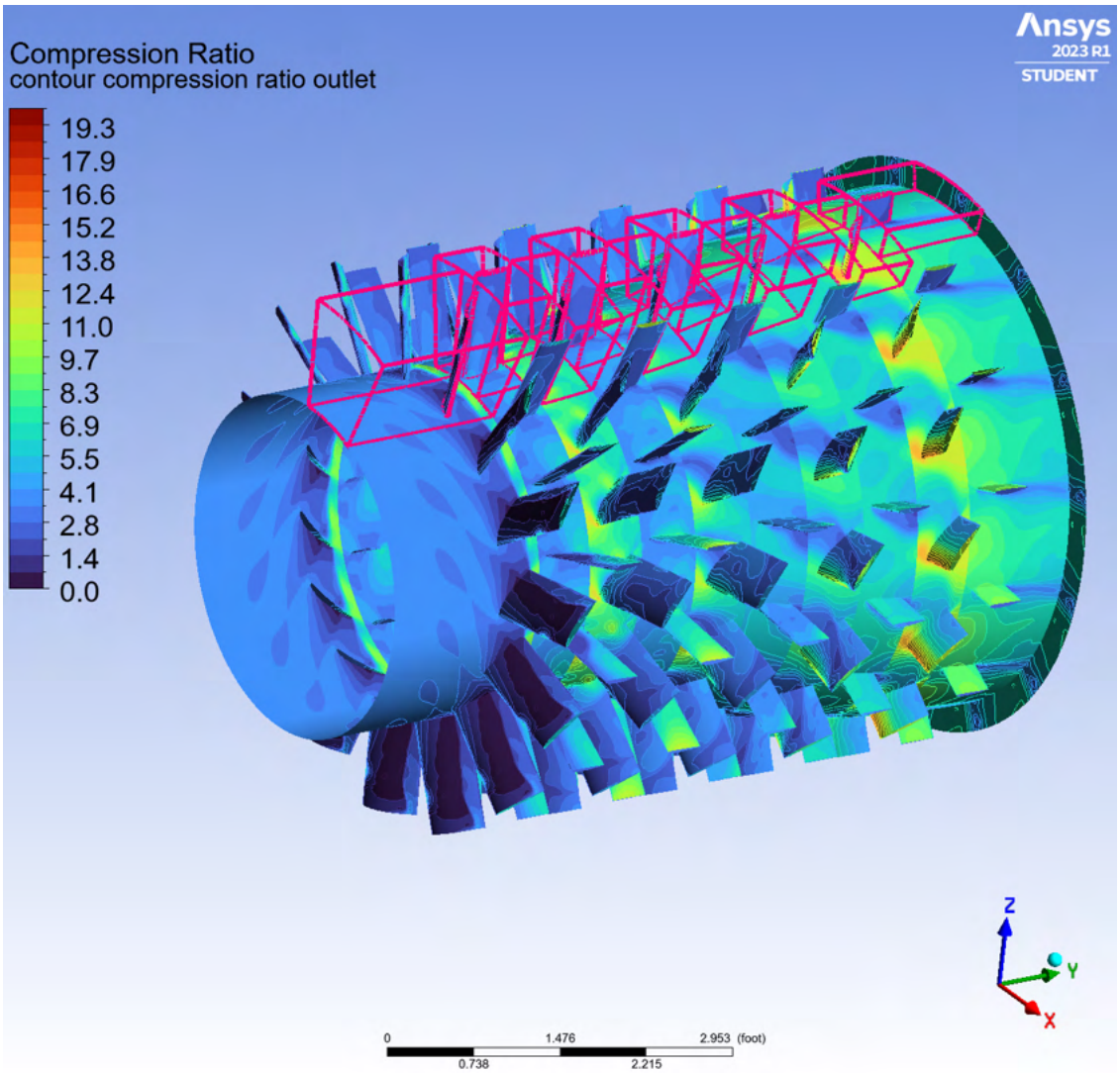

The compression ratio at standard temperature and pressure reaches a local maximum at 19.3. However, the area weighted average at the outlet only reaches a compression ratio of 2.75.

6.2 Operating Altitude (40,000 ft) Simulation Results

6.2.1 Temperature Contours

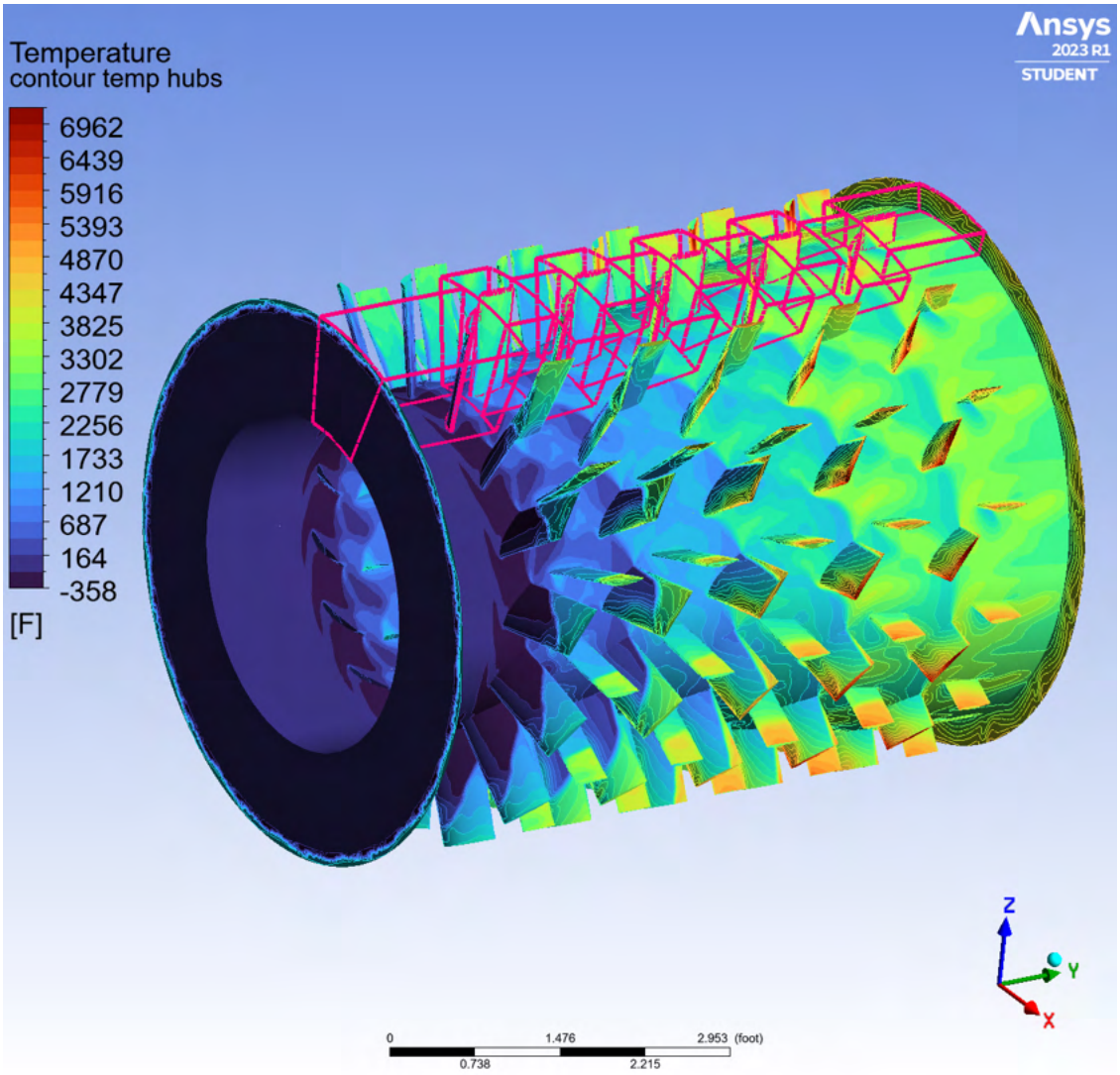

The area-weighted average outlet temperature at normal operating altitude is very high at 3562.9 °F, with an even higher local maximum of 7000 °F. This is above the melting point of the nickel alloy construction. However, this represents the temperature of the outlet air, and not the temperature at the surface. The temperature at the surface would be slightly lower thanks to conduction through the metal. Convection from the air during flight operations of the compressor would greatly decrease this temperature. Therefore, when running the compressor on the test stand, it is recommended that it is done in a wind tunnel to simulate the same convection effects and properly cool the engine.

6.2.2 Velocity Streamlines

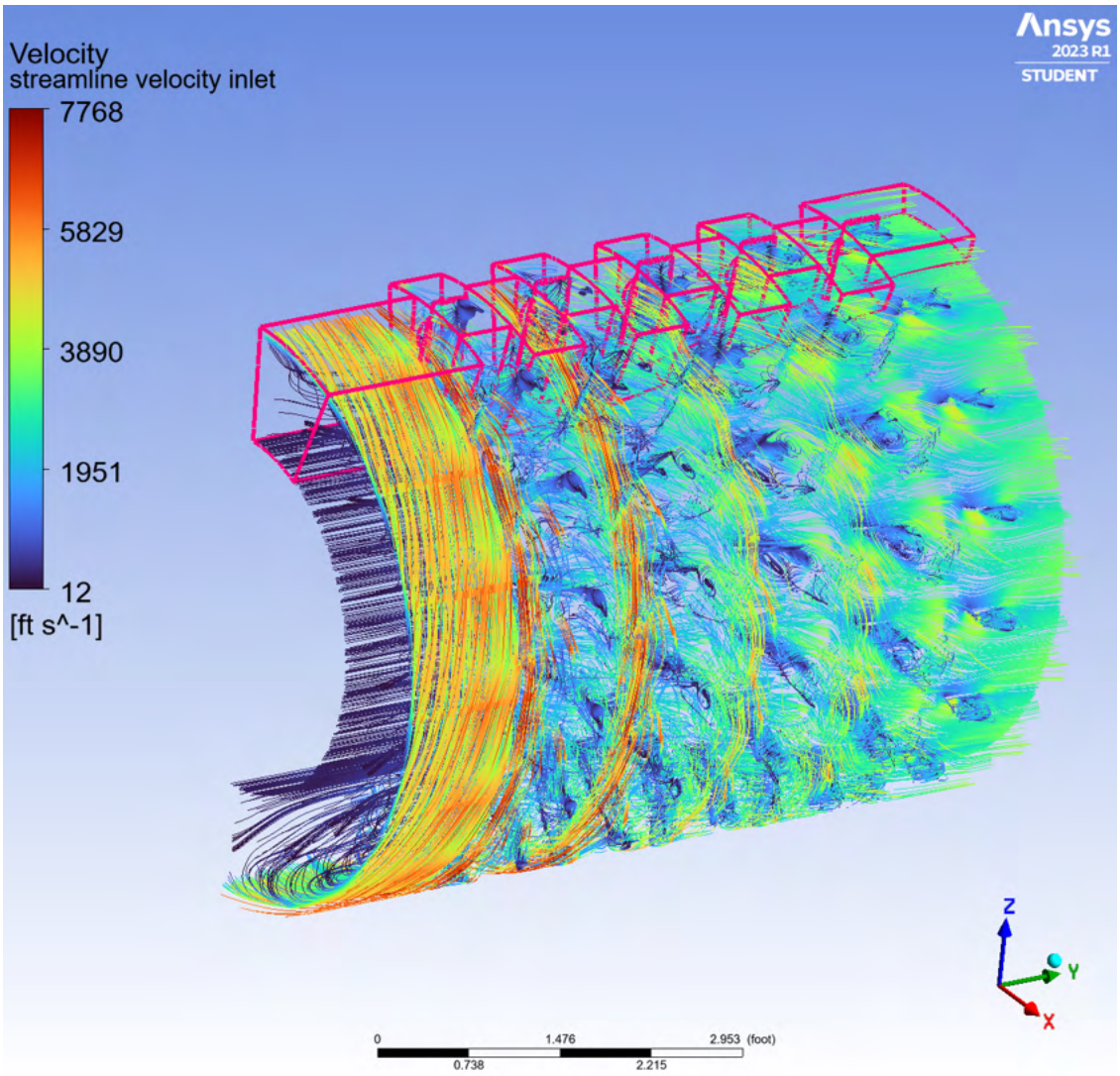

The velocity streamlines for the simulation at 40,000 feet is very similar to the that at STP. However, to help visualize the rotor stator interactions, the velocity in this plot is taken with respect to the rotors and expressed in the inertial frame as opposed to with respect to each stage. This is why the outer surface of the rotor at the inlet appears to be spinning with a very high velocity. As expected, the relative velocity is greatest at the inlet because the air does not yet have any velocity component tangent to the compressors outer surface. As the air starts spinning with the rotors, its velocity relative to the rotors decreases, which is why it drops significantly by the end.

6.2.3 Pressure Contours

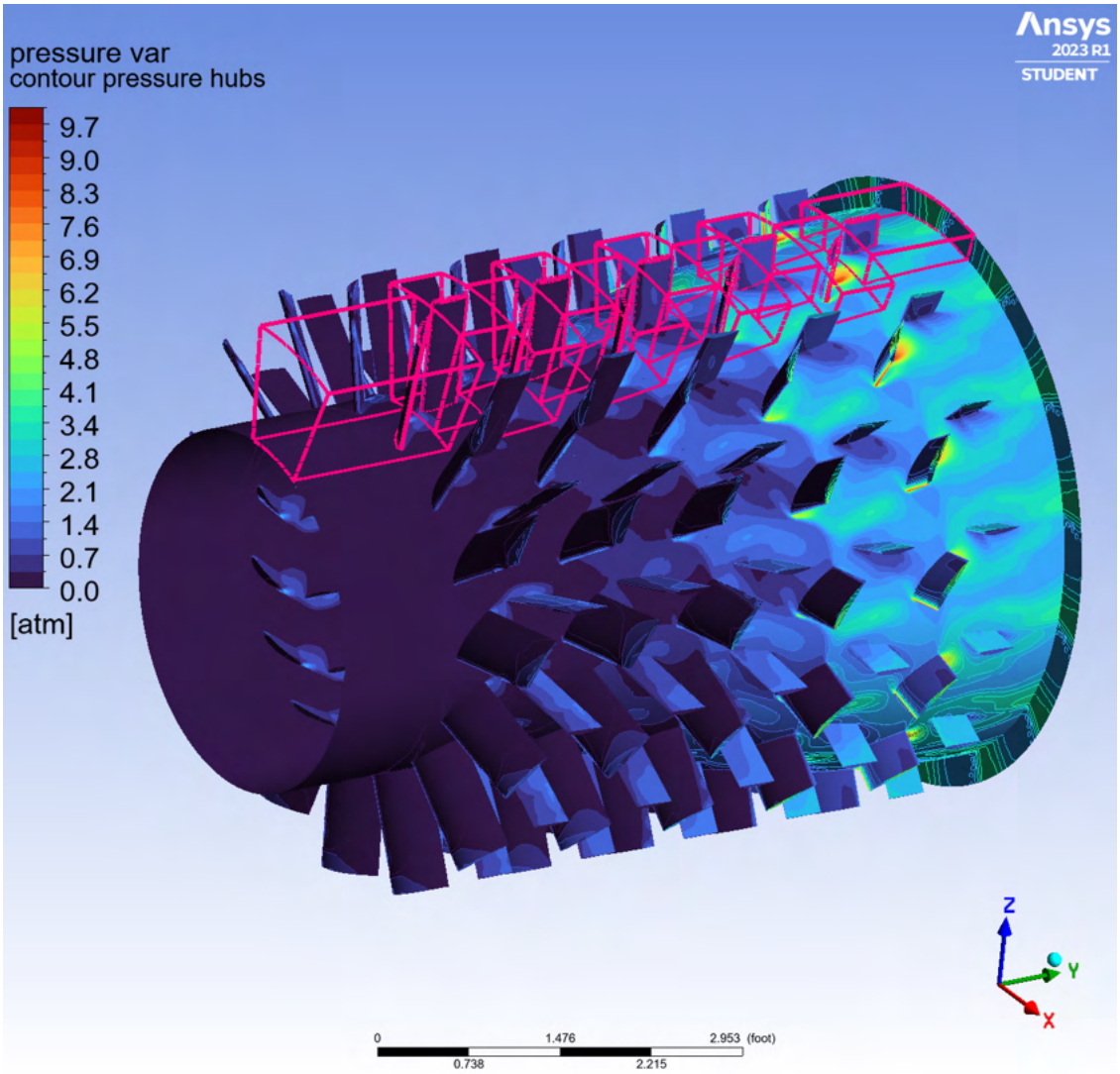

The pressure shown in this plot is gauge pressure. This is why the pressure is 0 at the inlet. The pressure difference from outlet to inlet is less than that of the STP case because the air is significantly less dense at high altitude. However, the compression ratio is still higher at the high altitude because the inlet pressure is also much higher at STP. There exists a high pressure concentration immediately behind the last rotor, which makes sense because the leading edge of an airfoil should always be of lower pressure to create lift, and the last rotor experiences the pressure increase from all the rotors before it.

6.2.4 Pressure Ratio

The pressure ratio, sometimes called the compression ratio, is calculated at standard temperature and pressure using Equation 26.

$$P_{ratio} = \frac{P_{out} + 0.1845atm}{0.1845atm} \tag{26}$$

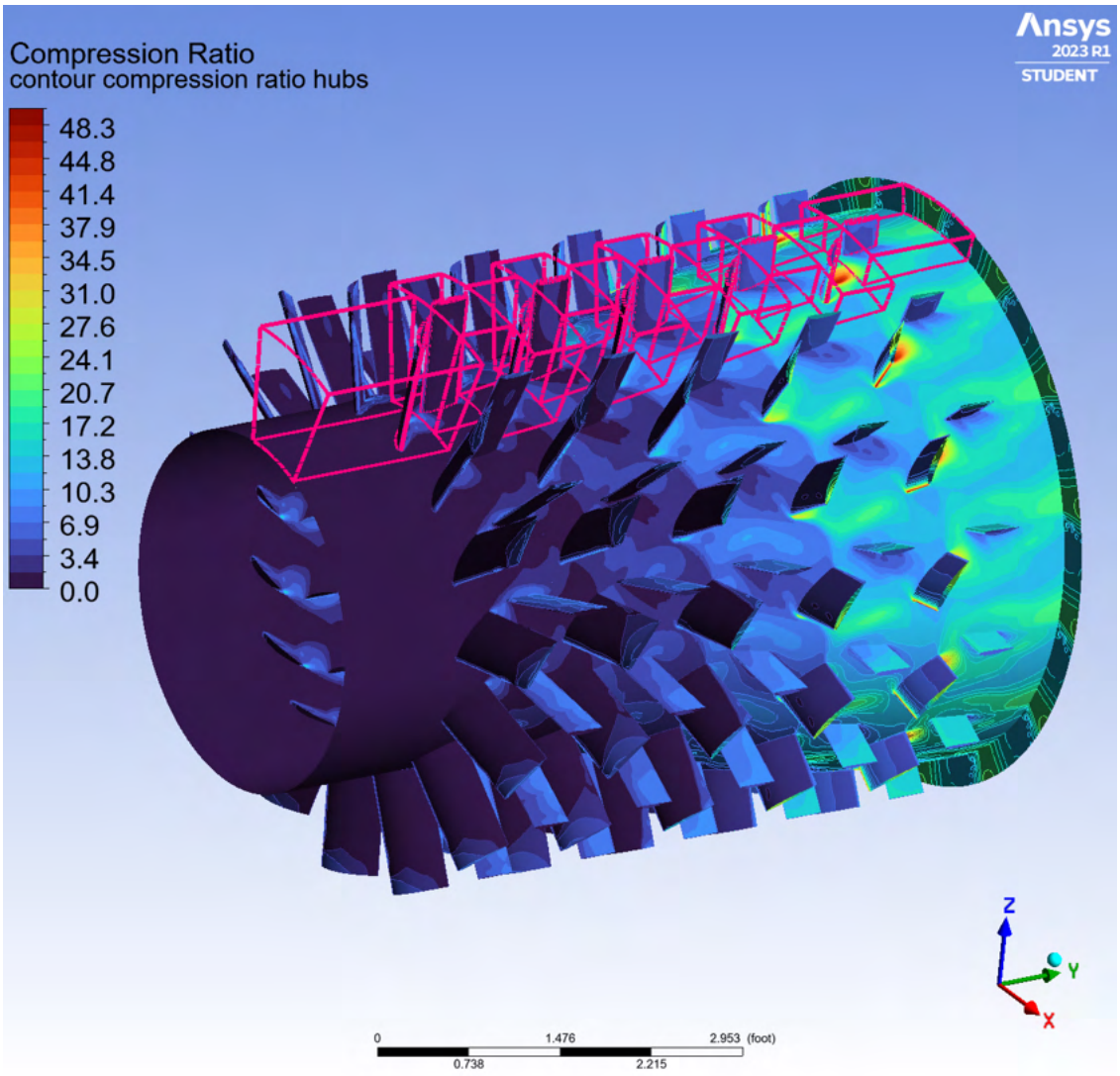

The compression ratio at standard temperature and pressure reaches a local maximum of 48. However, the area weighted average at the outlet only reaches a compression ratio of 15.9

6.2.5 Power Usage at each stage

The power usage is defined as the required torque times the rotational speed. Table 2 displays the power usage at each stage at the final rotational speed, 20,000 rpm.

	Stage 1	Stage 2	Stage 3	Stage 4	Stage 5
Power Usage (HP)	1953	2181	3898	6049	3970

Table 2: Power Usage of each stage

6.2.6 Compressor Efficiency

The compressor Efficiency is defined as

$$\epsilon = \frac{((T_{outlet} * (P_{ratio}^{(0.4/1.4)-1})}{(T_{outlet} - T_{inlet}))} * 100 \tag{27}$$

where

T_{outlet} = the total temperature at the outlet

T_{inlet} = the total temperature at the inlet

P_{ratio} = outlet pressure over inlet pressure

The compressor efficiency was obtained by setting up an expression in Fluent using Equation 28

$$\epsilon = \frac{T_{outlet} \times (P_{ratio}^{(0.4/1.4)} - 1)}{T_{outlet} - T_{inlet}} \times 100 \tag{28}$$

The compressor efficiency obtained from fluent was 21.01%. This matches very well with the hand calculation estimate of 20.1%.

6.2.7 Comparison to Hand Calculations

	40,000 Feet	Sea-Level
Area-averaged Outlet Pressure (atm)	3.4	5.4
Compression Ratio	15.9	6.4

Table 3: Tabulated Results after Averaging with the Aligned Rotor Stator Case

	Outlet Pressure	Outlet Temperature	Compressor Efficiency
40,000 Ft Simulation	3.4 atm	3562.9 F	21
Hand Calculation	4.059 atm	2062 F	20

Table 4: Comparison of Hand Calculation and Simulation Results

6.2.8 Extrapolation

When the model was increased to 20,000 rpm, the maximum pressure ratio at convergence at an operating altitude of 40,000 ft was under the design criteria at a ratio of 15.9. However, there is a clear trend that the pressure ratio increases with each consecutive rotor. This trend line shown in Figure 6.2 predicts that 1 additional rotor stage would be needed to reach the desired pressure ratio of 22:1. Therefore our final design will have a total of 6 rotor stages and 6 stator stages and is expected to achieve a final compression ratio of 22.8.

The temperature at the outlet of each blade shown in Figure 6.1 rises asymptotically slower with each additional blade. This is in stark contrast to the temperature increase when the rpm is increased. Although increasing the RPM would also meet the required pressure ratio, the temperature is already very high, and increasing the rpm more would cause the compressor to overheat and catch fire or melt itself. Therefore it is more desirable to modify the geometry as opposed to the RPM.

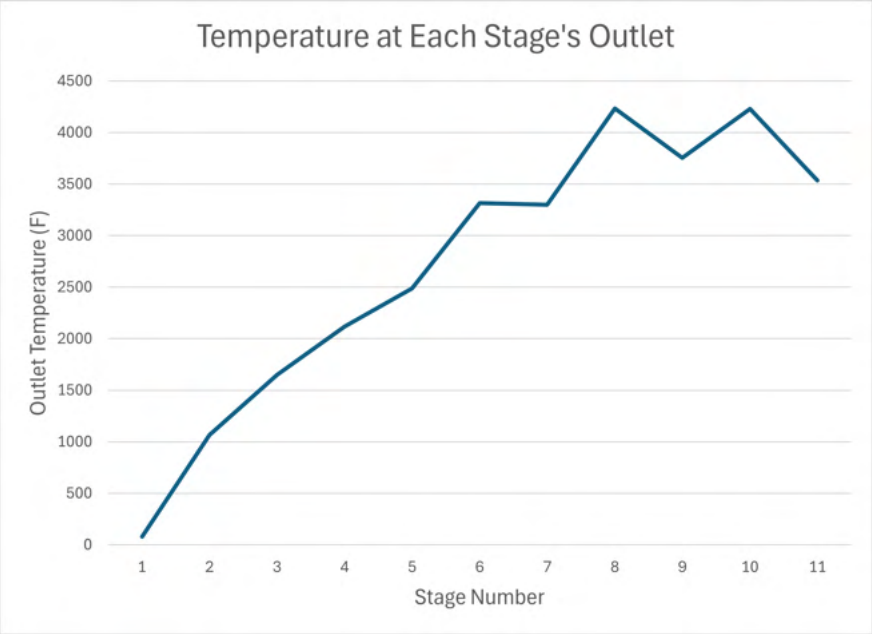

Figure 6.1: Temperature at the Outlet of Each Rotor/Stator Stage

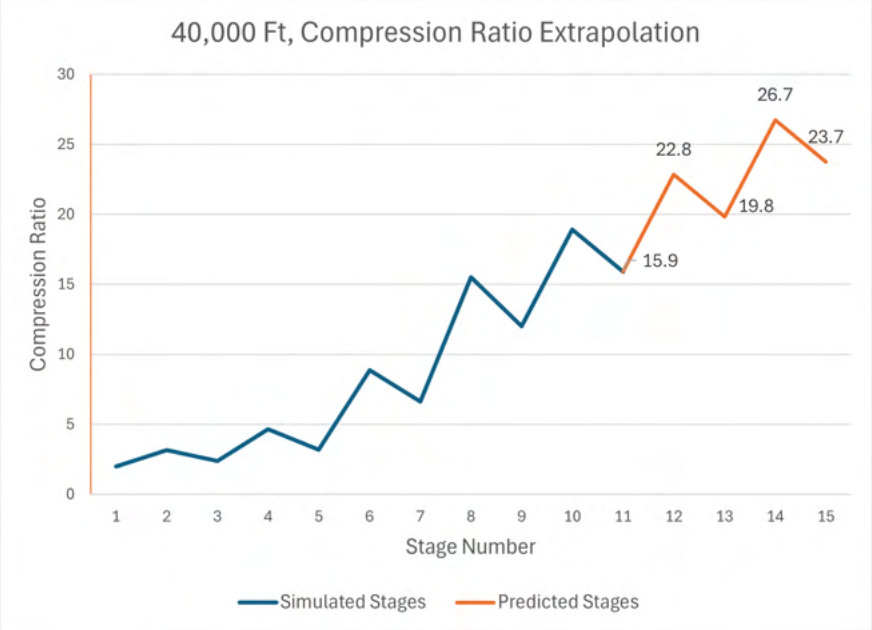

Figure 6.2: Compression Ratio at the Outlet of Each Rotor/Stator Stage. The yellow line labelled "Predicted Stages" was computed using the forecast tool in excel to predict the compression ratio if we were to add additional rotors or stators to the design. This is better than a line of best fit because it captures the oscillitory behavior governed by the fact that pressure and temperature is higher at the outlet of a rotor as opposed to at the outlet of a stator.

7 Final Remarks and Design Benefits

On jet engines, the high-pressure (HP) system, including the HP compressor and HP turbine, rotates at a speed called N2. Typical N2 speeds can be anywhere between 10,000 and 15,000 RPM. Special-purpose engines (such as military or surveillance engines) may even reach as high as 30,000 RPM. Our chosen operating speed of 20,000 RPM, aligns well with existing technology[4].

Our presented design is simple to run. Because it is axi-symmetric, the whole compressor can be simulated using only one row of blades. The fully mapped mesh keeps the element count down, and element quality high. The presented geometry reached the necessary compression ratio using only half of the maximum operating speed.

Future analysis would include running the model with all 12 stages to verify the extrapolation prediction, and experimenting with even more stages at lower rpm to lower the temperature and further optimize the efficiency. The simulation may also be more accurate at higher orders or when using a turbulence model. Further improvements could also be made to the geometry of the compressor to make each stage more tightly packed and to optimize the foil shape and angle of attack.

7.1 Design time estimate

Geometry: 3 hours
Meshing: 50 hours
Planning :7 hours
Setting Up: 20 hours
Solving : 100 hours
Write up: 20 hours
Total: **200 Hours**

References

[1] E. Toolbox, *Engineering toolbox*, 2023. [Online]. Available: `https://engineeringtoolbox.com`.

[2] NCEES, *Professional Engineer Mechanical Handbook*, 1.5. NCEES, 2023. [Online]. Available: `https://help.ncees.org/article/87-ncees-exam-reference-handbooks`.

[3] J. Anderson John D., *Fundamentals of Aerodynamics*, 6th ed. New York, NY: McGraw-Hill Education, 2017, ISBN: 978-1-259-12991-9.

[4] M. A. Johnston, *How do jet engines work?* 2024. [Online]. Available: `https://calaero.edu/how-do-jet-engines-work`.

[5] T. Baumeister, *Marks' Standard Handbook for Mechanical Engineers*, 12th ed. McGraw-Hill Education, 2017.

[6] T. L. Bergman, *Fundamentals of Heat and Mass Transfer*, Eighth. John Wiley and amp; Sons, Inc, 2017.

[7] *Matweb material data sheet*. [Online]. Available: `https://www.matweb.com`.

[8] I. ANSYS, *Ansys fluent user's guide*, Release 2023 R1, Jan. 2023.

[9] I. ANSYS, *Ansys fluent theory guide*, Release 2023 R1, Jan. 2023.

[10] J. W. Mitchell, *Fox and McDonald's Introduction to Fluid Mechanics*, 10th ed. Hoboken, NJ: John Wiley & Sons, Inc., 2020, ISBN: 978-1-119-61649-8.

A Appendix

A.1 Drawing of Final Design